Published in final edited form as:
Xenobiotica. 2012 August ; 42(8): 748–755. doi:10.3109/00498254.2012.662726.

Breast cancer resistant protein (BCRP/*ABCG$_2$*) localizes to the nucleus in glioblastoma multiforme cells

Prateek Bhatia[1], **Michel Bernier**[1], **Mitesh Sanghvi**[1], **Ruin Moaddel**[1], **Roland Schwarting**[2], **Anuradha Ramamoorthy**[1], and **Irving W. Wainer**[1,*]

[1]Laboratory of Clinical Investigation, National Institute on Aging, National Institutes of Health, Baltimore, MD 21224 USA.

[2]Department of Pathology, Cooper University Hospital, Camden, New Jersey 08103, USA

Abstract

1. The breast cancer resistant protein (BCRP), an ABC efflux transporter, plays a role in multiple drug resistance (MDR). Previous studies of the subcellular location of the ABC transporter P-glycorprotein indicated that this protein is expressed in nuclear membranes. This study examines the nuclear distribution of BCRP in seven human-derived glioblastoma (GBM) and astrocytoma cell lines.

2. BCRP expression was observed in the nuclear extracts of 6/7 cell lines. Using the GBM LN229 cell line as a model, nuclear BCRP protein was detected by immunoblotting and confocal laser microscopy. Importantly, nuclear BCRP staining was found in a subpopulation of tumor cells in a human brain GBM biopsy.

3. Mitoxantrone cytotoxicity in the LN229 cell line was determined with and without the BCRP inhibitor fumitremorgin C and after down-regulation of BCRP with small interfering RNA. Fumitremorgin C inhibition of BCRP increased mitoxantrone cytotoxicity with a ~7-fold reduction in the IC_{50} and this effect was further potentiated in the siRNA-treated cells.

4. In conclusion, BCRP is expressed in the nuclear extracts of select GBM and astrocytoma cell lines and in a human GBM tumor biopsy. Its presence in the nucleus of cancer cells suggests new role for BCRP in MDR.

Keywords

ABC transporters; multidrug resistance; mitoxantrone; small interfering RNA; confocal microscopy

INTRODUCTION

Glioblastoma multiforme (GBM) is one of the most aggressive forms of human astrocytoma as only ~10% of patients survive 5 years post diagnosis (for review see Salacz et al., 2011). One factor that contributes to this poor prognosis is acquired or innate multiple drug resistance (MDR), which decreases the therapeutic activity of a number of drugs used in the

*Corresponding Author Irving W. Wainer Ph.D., D.H.C. Bioanalytical Chemistry and Drug Discovery Section Laboratory of Clinical Investigation National Institute on Aging, NIH Biomedical Research Center 251 Bayview Blvd, Suite 100 Room 8B133 Baltimore, MD 21224 USA. Phone: 1-410-558-8498 Fax: 1-410-558-8409 wainerir@grc.nia.nih.gov.

Declaration of interest
The authors report no declaration of interest.

treatment of cancer. A key mechanism associated with MDR is the enhanced expression of ATP binding cassette (ABC) efflux transporters in cancer cells (Chang et al., 2003), which decrease intracellular drug accumulation, thereby reducing therapeutic effect. To date, 48 members of the ABC transporter gene family have been identified in humans (Chang, 2003; Doshi et al., 2011). While P-glycoprotein (Pgp/ABCB1) is the most studied ABC transporter, the breast cancer resistance protein (BCRP/ABCG2) has recently gained importance due to its widespread tissue distribution and role in the clinical MDR phenotype.

BCRP was initially cloned from a drug resistant human derived breast cancer cell line (MCF-7/AdrVp) (Doyle et al., 1998) and its expression has been reported in GBM cell lines and clinical specimen (Diestra et al., 2002; Bleau et al., 2009). Localized on the apical side of cells (Ishikawa et al., 2009), BCRP contributes to drug resistance through export of anticancer agents, including etoposide, doxorubicin, vinblastin, vincristin and mitoxantrone (MTX) (Robey et al., 2009). In addition, BCRP has been shown to play a role in protecting hematopoietic stem cells, and it appears that the expression profile of BCRP in human stem cells is significantly higher than that of Pgp (Yeboah et al., 2008). While ABC transporters are primarily localized in the cellular membrane, BCRP has been identified at subcellular sites like mitochondria (Takada et al., 2005; Solazzo et al., 2009) and the perinuclear region (Lemos et al., 2009) where it may act as a secondary site for efflux of its substrates.

In this study we investigated the expression and nuclear distribution of BCRP in seven human-derived glioblastoma and astrocytoma cell lines by Western blot analysis, using the human-derived breast cancer cell line MCF-7 as control. The results showed that BCRP was expressed both in nuclear and cytoplasmic/membraneous extracts in 6/7 experimental cell lines and only in the extranuclear fraction of the MCF-7 cell line. The LN229 cell line was chosen for further study and confocal microscopy confirmed the presence of nuclear BCRP. Importantly, BCRP staining was observed in a subpopulation of cells from a human GBM tumor biopsy. The down-regulation of BCRP by small interfering RNA (siRNA) or pharmacological inhibition of BCRP with fumitremorgin C (FTC) markedly increased the cytotoxic potential of MTX in LN229 and MCF-7 cells. However, the combined effect of BCRP siRNA plus FTC produced a MTX cytotoxic response that was greater than single intervention only in LN229 cells. These results indicate that the expression of nuclear BCRP in select glioblastoma cell lines and brain tumor cells from GBM biopsy may represent a new mechanism of MDR and pose new therapeutic challenges.

Materials and methods

Cell culture

The LN229, T98, A172, U87, U118, U138 glioblastoma cell lines and MCF-7 breast cancer cell line were purchased from American Type Culture Collection (Manassas, VA, USA). The 1321N1 astrocytoma cells were obtained from the European Collection of Cell Cultures (Sigma-Aldrich, St. Louis, MO, USA). The cell lines were cultured in Dulbecco's modified Eagle's medium (D-MEM) and Eagle's minimum essential medium (E-MEM) respectively, with 4.5 g glucose /L (Quality Biological Inc., Gaithersburg, MD, USA), supplemented with penicillin (25 U/ml), streptomycin (25 μg/ml), pyruvic acid and 5% foetal calf serum (Thermo Scientific, Waltham, MA, USA). Cells were maintained at 37°C in a humidified incubator with 5% CO_2.

Preparation of whole cell lysates

Cells at approximately 70 - 80% confluency were lysed on ice for 20 min in Tris-HCl [10mM, pH 7.4] containing 0.15M NaCl, 5mM EDTA, 1% Triton X-100, 1:500 dilution of a stock solution of protease inhibitor cocktail (#P2714, Sigma-Aldrich, St-Louis, MO, USA),

0.1M sodium orthovanadate and 0.1M dithiothreitol (Sigma-Aldrich). Insoluble material was removed by centrifugation (17,000×g for 20 min at 4°C) and the supernatant was collected and stored at -80°C until further analysis.

Nuclear fractionation

For experiments involving nuclear extract isolation, the NE-PER Nuclear and Cytoplasmic Extraction Reagents kit was used according to the manufacturer's protocol (Thermo Scientific).

Western blot analysis

The protein concentration of the lysates was measured with the BCA protein assay kit (Thermo Scientific) using BSA as the standard. An equal amount of 3X Laemlli sample buffer was added, and the samples (70 μg) were separated by electrophoresis using precast 4-12% gradient SDS-polyacrylamide gels (Invitrogen, Carlsbad, CA, USA) and transferred to polyvinylidene difluoride membranes using iBLOT (Invitrogen). The membranes were blocked with 5% dry non-fat milk in Tris-buffered saline with 0.1% Tween-20 and then probed with a number of primary mouse monoclonal antibodies. These include: anti-BCRP (clone BXP-21, 1:500 dilution; Alexis Biochemicals, Plymouth Meeting, PA, USA), anti-Pgp (C219, 1:500; Alexis Biochemicals, San Diego, CA, USA), anti-β-actin (1:5000 dilution; Abcam, Cambridge, MA, USA), anti-NFκB p65 (clone F-6, 1:5000 dilution; Santa Cruz Biotechnology, Inc., Santa Cruz, CA, USA), and anti-BRG-1 (clone G-7, 1:5000 dilution; Santa Cruz). This was followed by incubation with horseradish peroxidase-conjugated secondary antibodies. The ECL Western blotting detection system (Santa Cruz) was used for visualization.

BCRP knockdown by siRNA transfection

Subconfluent LN229 and MCF-7 cells were transfected with either a pool of three BCRP siRNA oligonucleotides (s18056, s18057 and s18058; Ambion, Austin, TX, USA) or a siRNA non-targeting control (4390844; Ambion), using forward transfection technique with Lipofectamine RNAiMAX™ (Invitrogen) according to the manufacturer's instructions. Briefly, 15 nM siRNA was mixed with 35 μL Lipofectamine RNAiMAX™ and was allowed to form a siRNA-Lipofectamine complex for 20 min at room temperature. Cells were harvested, resuspended in appropriate media without penicillin-streptomycin and seeded with the siRNA-Lipofectamine complex. After 48-72 h, the cells were assayed for BCRP knockdown.

Immunofluorescent confocal microscopy

LN229 cells (25×10^3 cells/well) and MCF-7 cells (15×10^3 cells/well) were seeded on a 4-well LabTek II CC2 chamber slide system with lid (Nalge Nunc International, Roskilde, Denmark) and allowed to grow for 24 h. The medium was replaced with serum-free medium for 2 h, after which the cells were washed twice with phosphate-buffered saline (PBS) and fixed with 4% formaldehyde (Sigma-Aldrich) at room temperature for 10 min. After fixing, the cells were washed twice with PBS, permeabilized with 0.2% Triton X-00 (Sigma-Aldrich) for 5 min, washed again with PBS, and then blocked with 8% BSA at room temperature for 1 h. The mouse monoclonal anti-BCRP (clone BXP-21; 1:500 dilution) and rabbit polyclonal anti-emerin (1:1000; Abcam) were diluted with 1% BSA and added to the cells for 12 h at 4°C. After three PBS washes, Alexa Fluor 488 conjugated goat anti-mouse and Alexa Fluor 568 conjugated goat anti-rabbit antibodies were added to the slides and the cells were incubated at room temperature for 1 h. The cells were washed three times with PBS, mounted in Prolong Gold antifade (Invitrogen) and cured for 24 h at room temperature in the dark. Images were taken using a Zeiss Meta 510 confocal microscope.

MTS assay

The non-radioactive CellTiter 96® Aqueous cell proliferation assay was performed according to the manufacturer's protocol (Promega, Madison, WI, USA). Briefly, cells were seeded in 96-well plates at a density of 3.5×10^3 cells/well and cultured for 24 h. Stock solutions of MTX (Sigma-Aldrich) and fumitremorgin C (FTC, Sigma-Aldrich) were prepared in DMSO, each at 1 mM. FTC is a fungal toxin that has been shown to reverse resistance to doxorubicin, MTX, and topotecan in BCRP-expressing cells at micromolar concentrations. MTX was diluted in cell culture medium with a maximum of 0.5% DMSO to each well. The concentrations of MTX were 0.5, 5, 50, 500, 1000, 2500 and 5000 nM. After 48 h incubation, 20 μl of 0.5 mg/ml of the tetrazolium compound MTS was added to each well and further incubated for 1 h. The absorbance was measured at 490 nm with a micro-plate reader (Thermo Scientific). Change in growth rate was calculated as follows: [A_{490nm} of treated cells/A_{490nm} of control cells].

Liquid chromatographic determination of the intracellular concentration of FTC

Sample preparation—LN229 cells (~25×10^3) were allowed to adhere on 12 well plates for 24 h. On the day of the experiment, the cell monolayer was washed twice with 1×PBS to get rid of any cellular debris. The cells were exposed to 5 μM FTC in a final volume of 1ml in 1×PBS. The plates were maintained at 37°C for 60 min in a non-CO_2 incubator, after which the medium (PBS) was collected and labeled as extracellular extract. The cell monolayer was washed once with 1×PBS to remove loosely associated FTC on the cell surface. The cells were then incubated with 100 μL of acetonitrile for protein precipitation. All extracts were centrifuged at 13000 RPM for 5 min at 4°C to get rid of insoluble material and then stored at -20°C until analysis.

HPLC analysis—A previously reported liquid chromatography (LC) method for the detection of FTC in plasma and tissue (Garimella *et al.*, 2004) was modified to quantify FTC in extracellular and intracellular extracts. The LC system consisted of a 1100 series liquid chromatography/mass selective detector (LC/MSD) (Agilent Technologies, Palo Alto, CA, USA) equipped with a photodiode-array (2 nm resolution) detector interfaced to a 250 MHz Kayak XA computer (Hewlett-Packard, Palo Alto, CA, USA) using ChemStation software (Rev B.10.00, Hewlett-Packard). The chromatographic separation was achieved using an Eclipse Plus C_{18} column (3.9×150 mm id, 4 μm particle size) (Agilent Technologies) with a C_{18} (4 mm length× 3 mm i.d.) guard column cartridge system (Phenomenex, Torrance CA, USA). The mobile phase consisted of an isocratic flow of ammonium acetate [10 mM, pH 4.0] modified with acetonitrile (70:30, v/v) delivered at a flow rate of 0.5 mL/min at room temperature. The samples (20 μl) were introduced into the LC column using an Agilent G1367A autosampler and the detection of FTC was accomplished with UV absorbance at λ = 225 nm. The total run time was 20 min. The quantification of FTC was accomplished using five-point calibration curves of 0.1, 0.25, 0.5, 0.75, 1 μM for intracellular FTC and 1, 2.5, 5, 10, 15 μM for its extracellular determination. The quantification of FTC was accomplished using the area ratios calculated using the FTC peak area of the calibrators divided by the peak area of 5 μM FTC, which was used as an external standard. Utilizing this approach the linearity of the determination of intracellular FTC was y=101.51x-5.9054, r^2=0.984 and for the extracellular FTC determination the results were y=48.171x-41.739, r^2=0.991.

Immunohistochemistry

Immunohistochemical staining was carried out using an established avidin-biotin complex indirect immuno-peroxidase method as described (Bain *et al.*, 1997; van Tellingen *et al.*, 2003). Routine biopsy specimens were retrospectively obtained from the Department of

Pathology at Cooper University Hospital and used with approval of the Cooper University Hospital Institutional Review Board. The specimens were cryostat sectioned at 7 μm onto polylysine coated slides, air dried, and stored at -70 °C. Immunohistochemical stains were performed on a fully automated Benchmark Ultra IHC stainer (Ventana Medical Systems, Tuscon, AZ, USA) to visualize BCRP using the mouse monoclonal anti-BCRP (clone BXP-21, 1:100 dilution).

Data analysis

The MTS assay data were fitted with a sigmoidal concentration-response curve using GraphPad Prism Version 4 (GraphPad Software, San Diego, CA, USA), and the IC_{50} values were determined using sigmoidal dose-response with a variable slope. The *p*-values were determined by the Student's t-test with Welch's correction. All experimental results were determined in triplicates. The number of independent experiments performed is described in each figure or table legend. Statistical analysis is described in the individual figure legend.

RESULTS

Nuclear expression of BCRP in human-derived GBM and astrocytoma cell lines

The expression of BCRP protein was analyzed by immunoblotting using BXP-21 as the primary antibody. This antibody has been reported to detect BCRP protein on immunoblots and is reactive with BCRP by flow cytometry and immunohistochemical techniques (Maliepaard et al., 2001; Minderman et al., 2002; Diestra et al., 2002; Lee et al., 2007). The human-derived breast adenocarcinoma cell line, MCF-7, was used as positive control as it has been previously demonstrated that BCRP is expressed in this cell line (Doyle et al., 1998). Western blot analysis using the whole cell lysate detected BCRP in the cell lysates of 6/7 experimental cell lines [LN229, T98, A172, 1321N1, U87, and U138] and in the control MCF-7 but not in the U118 cell lysates (data not shown).

To study the localization of BCRP, nuclear and cytosolic/membraneous fractions were isolated from the experimental cell lines and MCF-7 cells, and these fractions were probed by Western blot analysis (Figure 1A, B). The results demonstrate that BCRP was found in the extranuclear fraction of MCF-7 cells and 4 of the experimental cell lines. However, the nuclear fractions of 5 of experimental cell lines contained BCRP whereas the MCF-7 nuclear extracts were devoid of this transporter. In agreement with the findings of Baldini et al. (1995), Pgp was found in the nuclear preparations of a subset of cell lines (Figure 1A). The blots were reprobed for the presence of cytoplasmic marker p65Rel subunit of NF-κB to evaluate the purity of nuclear extracts (Figure 1A, B). While being positive for the nuclear marker BRG1, the nuclear fractions were devoid of p65Rel, confirming that during the fractionation process no leaking or cross-contamination occurred. Note that the signal associated with BRG1 and p65Rel was comparable in the cell lines used in this study.

Based on these evaluations we focused on the BCRP regulation in LN229 and MCF-7 cells. Transfection of both cell types with a pool of BCRP siRNAs led to a ~80% reduction in BCRP protein levels as compared to cells transfected with a control non-targeting siRNA (Figure 1C).

BCRP subcellular localization by immunofluorescence

Confocal immunofluorescence microscopy was used to further investigate the subcellular localization of BCRP in the LN229 and MCF-7 cell lines (Figure 2). Cytosolic/membraneous localization of BCRP was observed in both cell lines (Figure 2A, upper panels); however, there was significant nuclear localization of BCRP in the LN229 cells as indicated by the co-staining of emerin (Figure 2A, middle and bottom panels). In contrast,

BCRP staining could not be detected in MCF-7 cell nuclei, in agreement with the Western blot analysis. Vertical sections in the *x-z* and *y-z* planes of confocal images were generated from fixed LN229 cells and showed staining consistent with BCRP and emerin co-localization (Figure 2B, depicted in yellow). No detectable nuclear expression of BCRP was observed in MCF-7 cells, as there was a clear demarcation of BCRP and emerin staining without co-localization (Figure 2B). Cross-sectional quantification of the images indicated the signal intensity to be uniform in both sets of images.

Immunohistochemical analysis of BCRP expression in human tissue biopsies

The study of Diestra et al. [2002] clearly showed that BCRP is expressed in 129 out of 150 tumor samples including 5 out of 5 GBM tissue specimens. More recently, BCRP has been shown to be localized only in microvessel endothelium of human control brain (Aronica et al., 2005). The results from our immunohistochemical study indicated that BCRP was indeed expressed in microvessel endothelium and in the extranuclear compartment of glial cells in a human control brain tissue biopsy (Figure 3A). When tissue from a human breast tumor biopsy specimen was examined, a marked staining of BCRP was observed in the cytosolic/membraneous compartment, but no nuclear staining was found (Figure 3B). Immunohistochemical staining of a tissue biopsy sample from a human GBM tumor indicated the presence of BCRP in the extranuclear compartment and, most importantly, nuclear BCRP expression was observed in a subpopulation of tumor cells (Figure 3C).

Effect of BCRP inhibition and siRNA-mediated BCRP knockdown on MTX-induced cytotoxicity

The DNA intercalating agent MTX has been identified as a specific substrate of BCRP efflux activity (Volk et al., 2002), and previous studies have demonstrated that the cytotoxicity of MTX is directly related to its intracellular accumulation. FTC elicits specific, selective and potent inhibition of BCRP-mediated efflux of cytotoxic drugs, thereby increasing their intracellular concentrations (Rabindran et al., 2000). Because cellular accumulation of FTC has never been reported, we adapted a liquid chromatography assay for the detection of FTC in the intracellular compartment. When LN229 cells were incubated in the presence of 5 μM FTC, the drug readily accumulated in the cytosol (Figure 4). The intracellular concentration of FTC was determined to be 32 μM after adjusting for the intracellular volume (0.375 μl for 50×10^3 cells (Chan *et al.*, 1982)). Therefore, it is likely that FTC will also be able to inhibit the export function of BCRP located within the nuclear membrane.

Using a cell proliferation assay, the growth inhibitory activity of MTX was determined in the absence or presence of FTC (5μM) in LN229 cells following down-modulation of BCRP protein by siRNA. The IC_{50} of MTX in a panel of human glioma cell lines has been previously reported as ~0.5 μM (Martin et al., 2009). Therefore, we chose this concentration of MTX to evaluate the chemoresistance index after pharmacological inhibition and/or silencing of BCRP (Figure 5A). The results indicated that the MTX-induced growth inhibition was increased 1.24 ± 0.08-fold upon addition of FTC to LN229 cells transfected with a negative, non-silencing control siRNA. We then compared the ability of FTC to potentiate MTX cytotoxicity in LN229 cells transfected with BCRP siRNA. The anti-proliferative effects of MTX in BCRP-knockdown cells was increased by 1.80 ± 0.11-fold, and reached 3.04 ± 0.22-fold when combined with FTC (Figure 5A). The additive effect of FTC in 'BCRP silenced' cells is consistent with the fact that the siRNA-mediated BCRP down-regulation was at best 70-80% (Figures 1C and 2A) and, therefore, subject to FTC inhibition. As anticipated, the addition of FTC potentiated the anti-proliferative effects of MTX in MCF-7 cells, passing from ~45% to 75% growth inhibition relative to vehicle control. However, the addition of FTC to BCRP siRNA-treated MCF-7 cells failed to

potentiate MTX cytotoxicity over that observed with cells transfected with control siRNA and co-incubated with FTC plus MTX (data not shown). This profile was remarkably different as compared to LN229 cells.

In the control siRNA-transfected LN229 cells, the MTX effect was fitted to a single concentration dependent sigmoidal curve (Figure 5B) and the calculated IC_{50} value was 476 ± 2 nM. When the study was repeated with 5μM FTC in the incubation media, the data was best fitted to a bimodal model using MTX concentrations ranging from 0.5 to 50 nM and 50 to 5000 nM. Using this approach the two MTX IC_{50} values were 24.9 ± 0.4 nM (0.5 to 50 nM) and 582 ± 1 nM (50 to 5000 nM). The same bimodal model was used to analyze the data from the effect of 5μM FTC in the BCRP siRNA-transfected cells. The IC_{50} values of MTX were 0.9 ± 0.0 nM (0.5 to 50 nM) and 647 ± 1 nM (50 to 5000 nM). These results indicate that the potentiating effect of FTC on MTX-mediated inhibition of cell growth (Figure 5) stemmed from the inhibition of BCRP and that reduction of BCRP expression by siRNA increased the observed effectiveness of FTC.

DISCUSSION

Effective chemotherapy of GBM is limited due to a multitude of factors. Many anti-cancer agents fail to cross the blood brain barrier (BBB) as they are not lipophilic and those that do penetrate the BBB are often effluxed by ABC transporters such as Pgp, MRP1, MRP2 and BCRP. One clinical strategy to overcome transporter-mediated MDR is to co-administer ABC transporter inhibitors with the objective of increasing intracellular concentrations of the chemotherapeutic agents and achieving required therapeutic exposure. This approach is predicated on the assumption that ABC transporter proteins are located primarily on cellular membranes and that the primary goal is to increase the cytosolic concentrations of the cytotoxic agents. However, the data from this study suggest that overcoming a BCRP-related MDR phenotype may be a more complex task.

In this study, we have demonstrated the presence of BCRP in the nuclear extracts of a number of human-derived glioblastoma and astrocytoma cell lines. This finding is consistent with previous reports showing that BCRP can be found in intracellular compartments, such as the mitochondria (Takada et al., 2005) and the perinuclear region (Lemos et al., 2009). Here, we provide the first report of BCRP being localized specifically to the nucleus of GBM cells. In silico analysis of human BCRP protein sequence (Swiss-Prot entry: Q9UNQ0) indicated the presence of a cluster of 4 lysine residues at position 357-360. This motif (^{357}KKKK^{360}), present in all three BCRP variants, has been identified as a putative nuclear localization sequence (NLS), which tags a protein for nuclear import through interaction with specific receptors at nuclear pores (Nardozzi et al., 2010). Interestingly, BCRP is the target of phosphorylation at Thr362 by Pim-1 kinase (Xie et al., 2008), which could have a profound impact on its cellular redistribution. Moreover, the protein Ser/Thr kinase, Akt, regulates the cell surface expression of BCRP by promoting its phosphorylation (Takada et al., 2005). Whether nuclear BCRP import is dependent of the phosphorylation on Thr362 is unclear. Alternatively, phosphorylation of a yet unknown putative site may upregulate importin-dependent BCRP nuclear import. Such phosphorylation may elicit conformational change within BCRP to enable better or reduced access to the nuclear import machinery. It is tempting to speculate that nuclear import of BCRP could be mediated, at least in part, through cell type- or region-specific activation of a discrete pool of kinase(s) acting on BCRP.

The data from the immunohistochemical studies of human tissue biopsies indicate that the nuclear expression of BCRP is a clinically relevant issue. The results also shed some light on the mechanisms associated with the development of the ABC transporter-associated

MDR phenotype. In a recent review, Moitra and co-workers (Moitra et al., 2011) present four potential models of this phenomenon: 1) Conventional model in which a population of the tumour cells have the MDR phenotype before initiation of chemotherapy; 2) Cancer stem cell model in which a small population of tumor stem cells express the MDR phenotype before chemotherapy; 3) Acquired-resistance stem cell model in which chemotherapy induces genetic changes that produce the MDR phenotype; 4) Intrinsic resistance model in which the tumor has intrinsic resistance to chemotherapy. The identification of BCRP nuclear expression in a subpopulation of tumor cells in a human GBM biopsy specimen supports the first two models.

We believe that the nuclear expression of BCRP has functional consequences with regard to the removal of cytotoxic drugs from the nucleus. Variants of BCRP have been shown to respond differentially to its substrates (Kondo et al., 2004), and, therefore, discrete variations in BCRP transcript sequences may contribute to cell type-specific differences in the magnitude of BCRP's export function (Ni et al., 2010). Moreover, the presence of Pgp on the nuclear membrane indicates that removal of MTX from the nucleus is presumably mediated by nuclear BCRP (this study), Pgp (Baldini et al., 1995) or other proteins involved in the nuclear-cytoplasmic trafficking and compartmentalization of drugs.

In conclusion, the expression of BCRP in the nuclei of glioblastoma and astrocytoma cell lines represents a potentially new mechanism of MDR. Insertion of BCRP within the nuclear envelope may alter the conformation and/or function of the protein as well as the efficacy of chemotherapeutic drugs relative to the transporter located at the plasma membrane. Interaction with the various components of cellular membranes has been suggested as the source of functional differences in β_2 adrenergic receptors expressed in different cell lines (Audet and Bouvier, 2008). The presence of BCRP and other ABC transporters on the nuclear membrane poses new therapeutic challenges in the treatment of MDR tumors and indicate that the development of specific inhibitors of nuclear ABC transporters may be required.

Acknowledgments

We thank Dr. Fred E. Indig and Sarah Subaran from the Research Resources Branch, NIA-NIH, for assistance with confocal microscopy imaging, and Otis Defreitas from the Dept. of Pathology, Cooper University Hospital, for immunohistochemical staining of various human biopsies. This work was supported by the Intramural Research Program of the National Institute on Aging, NIH.

The abbreviations used are

GBM	glioblastoma multiforme
ABC	ATP binding cassette
MDR	multiple drug resistance
BCRP	breast cancer resistance protein
Pgp	P-glycoprotein
MRP	multidrug resistance protein
BBB	blood-brain barrier
PBS	phosphate-buffered saline
siRNA	silencing RNA

MTS	3-(4,5-dimethylthiazol-2-yl)-5-(3-carboxymethoxyphenyl)-2-(4-sulfophenyl)-2H-tetrazolium, inner salt
MTX	mitoxantrone
FTC	fumitremorgin C

References

Aronica E, Gorter JA, Redeker S, van Vliet EA, Ramkema M, Scheffer GL, Scheper RJ, van der Valk P, Leenstra S, Baayen JC, Spliet WG, Troost D. Localization of breast cancer resistance protein (BCRP) in microvessel endothelium of human control and epileptic brain. Epilepsia. 2005; 46:849–57. [PubMed: 15946326]

Audet M, Bouvier M. Insights into signaling from the β2-adrenergic receptor structure. Nat Chem Biol. 2008; 4:397–403. [PubMed: 18560432]

Bain LJ, McLachlan JB, LeBlanc GA. Structure-activity relationships for xenobiotic transport substrates and inhibitory ligands of P-glycoprotein. Environ Health Perspect. 1997; 105:812–8. [PubMed: 9347896]

Baldini N, Scotlandi K, Serra M, Shikita T, Zini N, Ognibene A, Santi S, Ferracini R, Maraldi NM. Nuclear immunolocalization of P-glycoprotein in multidrug-resistant cell lines showing similar mechanism of doxorubicin distribution. Eur J Cell Biol. 1995; 68:226–39. [PubMed: 8603675]

Bleau AM, Huse JT, Holland EC. The ABCG2 resistance network of glioblastoma. Cell Cycle. 2009; 8:2936–44. [PubMed: 19713741]

Chan PH, Kerlan R, Fishman RA. Intracellular volume of osmotically regulated C6 glioma cells. J Neurosci Res. 1982; 8:67–72. [PubMed: 7175979]

Chang G. Multidrug resistance ABC transporters. FEBS Lett. 2003; 555:102–5. [PubMed: 14630327]

Diestra JE, Scheffer GL, Català I, Maliepaard M, Schellens JHM, Scheper RJ, Germà-Lluch JR, Izquierdo MA. Frequent expression of the multi-drug resistance-associated protein BCRP/MXR/ABCP/ABCG2 in human tumours detected by the BXP-21 monoclonal antibody in paraffin-embedded material. J Pathol. 2002; 198:213–9. [PubMed: 12237881]

Doshi R, Gutmann DA, Khoo YS, Fagg LA, van Veen HW. The choreography of multidrug export. Biochem Soc Trans. 2011; 39:807–11. [PubMed: 21599652]

Doyle LA, Yang W, Abruzzo LV, Krogmann T, Gao Y, Rishi AK, Ross DD. A multidrug resistance transporter from human MCF-7 breast cancer cells. Proc Natl Acad Sci U S A. 1998; 95:15665–70. [PubMed: 9861027]

Garimella TS, Ross DD, Bauer KS. Liquid chromatography method for the quantitation of the breast cancer resistance protein ABCG2 inhibitor fumitremorgin C and its chemical analogues in mouse plasma and tissues. J Chromatogr B Analyt Technol Biomed Life Sci. 2004; 807:203–8.

Ishikawa T. The role of human ABC transporter ABCG2 (BCRP) in pharmacotherapy. Adv Drug Deliv Rev. 2009; 61:1–2. [PubMed: 19124052]

Kondo C, Suzuki H, Itoda M, Ozawa S, Sawada J, Kobayashi D, Ieiri I, Mine K, Ohtsubo K, Sugiyama Y. Functional analysis of SNPs variants of BCRP/ABCG2. Pharm Res. 2004; 21:1895–903. [PubMed: 15553238]

Lee G, Babakhanian K, Ramaswamy M, Prat A, Wosik K, Bendayan R. Expression of the ATP-binding cassette membrane transporter, ABCG2, in human and rodent brain microvessel endothelial and glial cell culture systems. Pharm Res. 2007; 24:1262–74. [PubMed: 17380269]

Lemos C, Kathmann I, Giovannetti E, Calhau C, Jansen G, Peters GJ. Impact of cellular folate status and epidermal growth factor receptor expression on BCRP/ABCG2-mediated resistance to gefitinib and erlotinib. Br J Cancer. 2009; 100:1120–7. [PubMed: 19277036]

Maliepaard M, Scheffer GL, Faneyte IF, van Gastelen MA, Pijnenborg ACLM, Schinkel AH, van de Vijver MJ, Scheper RJ, Schellens JHM. Subcellular localization and distribution of the breast cancer resistance protein transporter in normal human tissues. Cancer Res. 2001; 61:3458–64. [PubMed: 11309308]

Martin V, Xu J, Pabbisetty SK, Alonso MM, Liu D, Lee OH, Gumin J, Bhat KP, Colman H, Lang FF, Fueyo J, Gomez-Manzano C. Tie2-mediated multidrug resistance in malignant gliomas is associated with upregulation of ABC transporters. Oncogene. 2009; 28:2358–63. [PubMed: 19421150]

Minderman H, Suvannasankha A, O'Loughlin KL, Scheffer GL, Scheper RJ, Robey RW, Baer MR. Flow cytometric analysis of breast cancer resistance protein expression and function. Cytometry. 2002; 48:59–65. [PubMed: 12116365]

Moitra K, Lou H, Dean M. Multidrug efflux pumps and cancer stem cells: Insights into multidrug resistance and therapeutic development. Clin Pharmacol Ther. 2011; 89:491–502. [PubMed: 21368752]

Nardozzi JD, Lott K, Cingolani G. Phosphorylation meets nuclear import: a review. Cell Commun Signal. 2010; 8:32. [PubMed: 21182795]

Ni Z, Bikadi Z, Rosenberg MF, Mao Q. Structure and function of the human breast cancer resistance protein (BCRP/ABCG2). Curr Drug Metab. 2010; 11:603–17. [PubMed: 20812902]

Rabindran SK, Ross DD, Doyle LA, Yang W, Greenberger LM. Fumitremorgin C reverses multidrug resistance in cells transfected with the breast cancer resistance protein. Cancer Res. 2000; 60:47–50. [PubMed: 10646850]

Robey RW, To KK, Polgar O, Dohse M, Fetsch P, Dean M, Bates SE. ABCG2: a perspective. Adv Drug Deliv Rev. 2009; 61:3–13. [PubMed: 19135109]

Salacz ME, Watson KR, Schomas DA. Glioblastoma: Part I. Current state of affairs. Mo Med. 2011; 108:187–94. [PubMed: 21736079]

Solazzo M, Fantappiè O, D'Amico M, Sassoli C, Tani A, Cipriani G, Bogani C, Formigli L, Mazzanti R. Mitochondrial expression and functional activity of breast cancer resistance protein in different multiple drug-resistant cell lines. Cancer Res. 2009; 69:7235–42. [PubMed: 19706772]

Takada T, Suzuki H, Gotoh Y, Sugiyama Y. Regulation of the cell surface expression of human BCRP/ABCG2 by the phosphorylation state of Akt in polarized cells. Drug Metab Dispos. 2005; 33:905–9. [PubMed: 15843490]

van Tellingen O, Buckle T, Jonker JW, van der Valk MA, Beijnen JH. P-glycoprotein and Mrp1 collectively protect the bone marrow from vincristine-induced toxicity in vivo. Br J Cancer. 2003; 89:1776–82. [PubMed: 14583783]

Volk EL, Farley KM, Wu Y, Li F, Robey RW, Schneider E. Overexpression of wild-type breast cancer resistance protein mediates methotrexate resistance. Cancer Res. 2002; 62:5035–40. [PubMed: 12208758]

Xie Y, Xu K, Linn DE, Yang X, Guo Z, Shimelis H, Nakanishi T, Ross DD, Chen H, Fazli L, Gleave ME, Qiu Y. The 44-kDa Pim-1 Kinase Phosphorylates BCRP/ABCG2 and Thereby Promotes Its Multimerization and Drug-resistant Activity in Human Prostate Cancer Cells. J Biol Chem. 2008; 283:3349–56. [PubMed: 18056989]

Yeboah D, Kalabis GM, Sun M, Ou RC, Matthews SG, Gibb W. Expression and localisation of breast cancer resistance protein (BCRP) in human fetal membranes and decidua and the influence of labour at term. Reprod Fertil Dev. 2008; 20:328–34. [PubMed: 18255023]

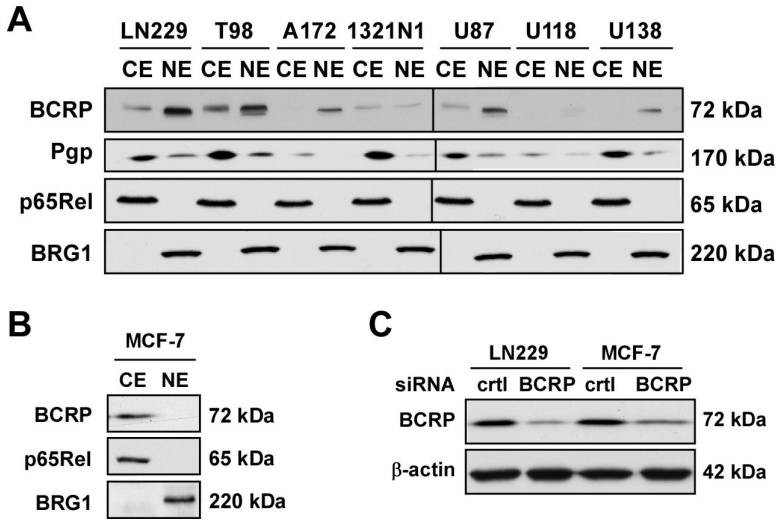

Figure 1. Detection of BCRP by immunoblot analysis

(A, B) Cytoplasmic/membraneous (CE) and nuclear (NE) extracts were prepared from the indicated human-derived cell lines and subjected to Western blot analysis for the detection of BCRP and Pgp using specific primary antibodies. The membranes were reprobed with antibodies against the cytosolic marker, p65Rel [a subunit of NFκB], and the nuclear marker BRG1 to confirm the quality of the nuclear extracts. The black line shown in Fig. 1A indicates that two sets of samples [(LN229..1321N1) and (U87..U138)] were ran on separate SDS-PAGE gels. Both gels were transferred to PVDF membranes, immunoblotted and developed with ECL at the same time. Images from the scanned films were then cropped and merged into a single image. (C) LN229 and MCF-7 cells were transfected with either a non-targeting control siRNA or BCRP siRNAs for 24 h, after which cells were lysed and processed for the detection of BCRP and β-actin by immunoblot analysis. Similar results were obtained in three independent experiments. The molecular mass markers (in kDa) are shown on the right.

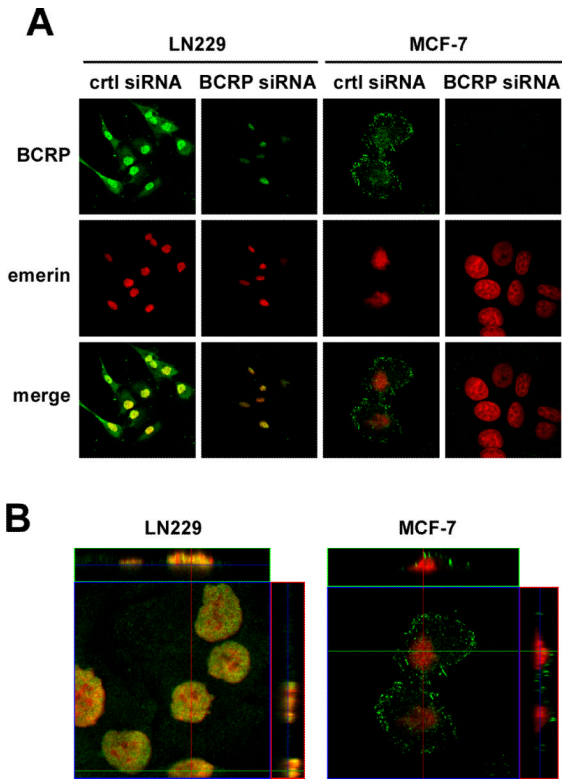

Figure 2. Cellular distribution of BCRP by confocal laser microscopy

LN229 cells and MCF-7 cells were transfected with control and BCRP siRNAs for 24 h. Cells were then fixed and immunolabeled with monoclonal anti-BCRP (green, upper panels) and polyclonal anti-emerin (red, middle panels) antibodies. Merge images are shown in the bottom panels. Areas of nuclear co-localization between BCRP and emerin appear in yellow in LN229 cells, which were absent in MCF-7 cells. Similar results were obtained in 3 independent experiments. (B) Vertical sections in the *XY* and *XZ* planes of confocal images from LN229 and MCF-7 cells tranfected with control siRNA. Magnification 40X.

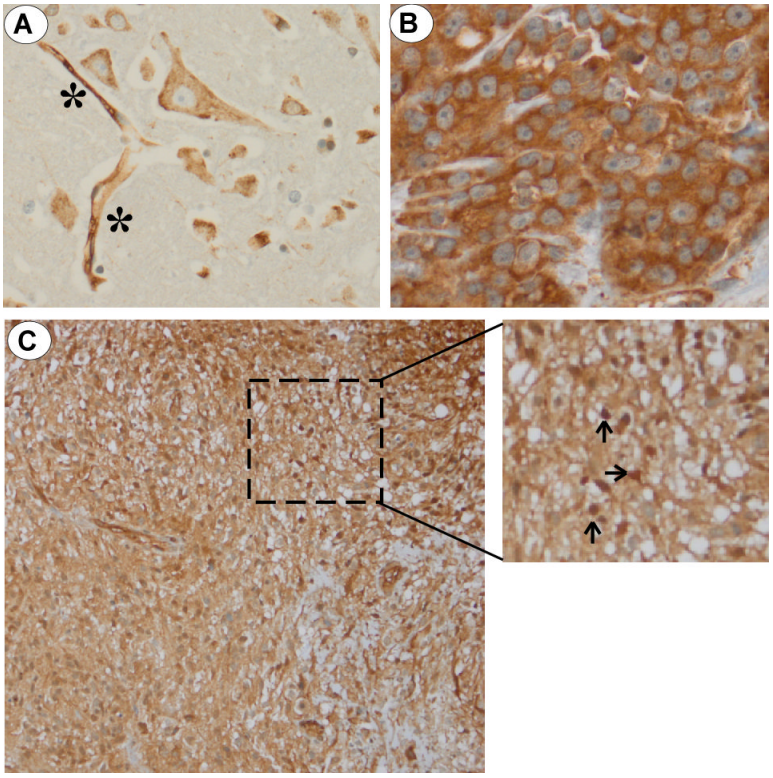

Figure 3. Expression and localization of BCRP in human brain tumor biopsy specimens

(A) Immunohistochemical analysis of BCRP in healthy, control human brain biopsy. BCRP staining of brain endothelial cells (denoted as *) and significant cytoplasmic/membraneous expression without nuclear expression of BCRP in brain glial cells; (B) A strong BCRP signal was observed in the cytoplasmic/membraneous compartment of a human breast cancer specimen. No nuclear BCRP staining was noted; (C) Biopsy GBM specimen at low (200X) and high (400X) magnification (inset) demonstrating nuclear BCRP staining in a subpopulation of tumor cells (denoted by arrows).

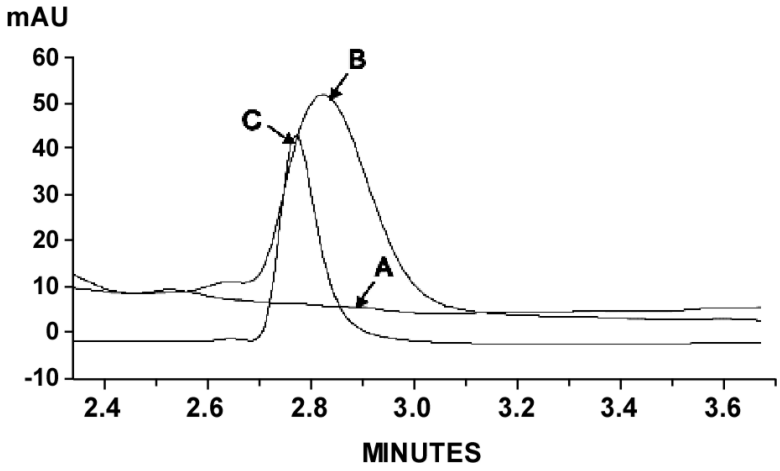

Figure 4. Detection of FTC by UV-HPLC

The chromatographic separation of FTC was accomplished with HPLC-UV (225 nm). Intracellular sample from LN229 cells treated with vehicle (A) was spiked with 5 μM FTC (B). (C) Intracellular sample from FTC-treated LN229 cells.

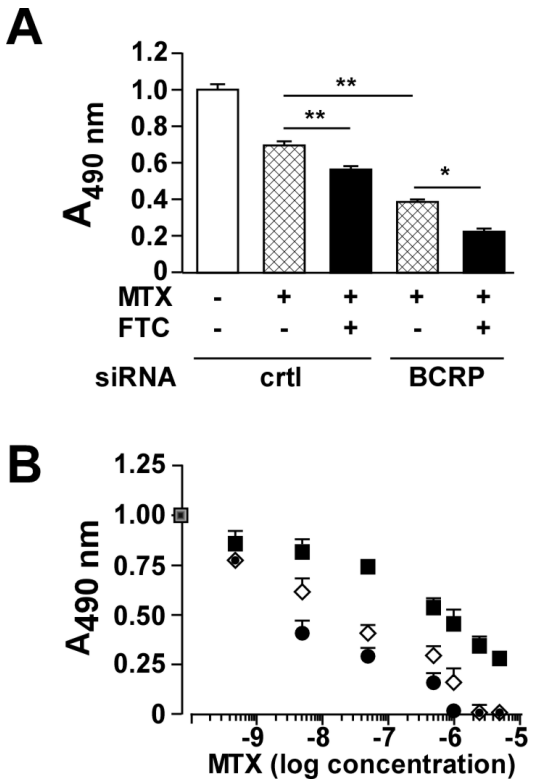

Figure 5. Role of BCRP in LN229 cell proliferation

(A) LN229 cells were transfected with control or BCRP siRNA for 24 h followed by the addition of 500 nM MTX in the absence or presence of 5 μM FTC for 48 h. A cell proliferation colorimetric assay based on MTS reduction was then performed. Values are means ± SEM from 3 independent experiments performed in triplicate. Statistical analysis by ANOVA with Dunnett's Multiple comparison test was performed, where *- $p < 0.05$; **- $p < 0.01$. (B) Control siRNA-transfected LN229 cells were incubated with the indicated concentrations of mitoxantrone (MTX) in the absence (filled square) or the presence of 5μM fumitremorgin C (FTC) (open diamond) for 48 h. Another group consisted of BCRP siRNA-treated LN229 cells incubated with MTX plus FTC (filled circle). Values are means ± SEM from 3 independent experiments performed in triplicate.